

# Surfactant-induced healing of tough hydrogels formed via hydrophobic interactions

Aslihan Argun · Melek Pamuk Algi ·  
Deniz C. Tuncaboğlu · Oguz Okay

Received: 12 September 2013 / Revised: 2 November 2013 / Accepted: 6 November 2013 / Published online: 21 November 2013  
© Springer-Verlag Berlin Heidelberg 2013

**Abstract** Different reversible molecular interactions have been used in the past few years to generate self-healing in synthetic hydrogels. However, self-healing hydrogels synthesized so far suffer from low mechanical strength which may limit their use in any stress-bearing applications. Here, we present a simple technique to heal mechanically strong polyacrylamide hydrogels formed via hydrophobic interactions between stearyl groups. A complete healing in the hydrogels was achieved by the treatment of the damaged areas with an aqueous solution of wormlike sodium dodecyl sulfate micelles. The micelles in the healing agent solubilize the hydrophobes in the cut surfaces, so that they easily find their partners in the other cut surface due to the hydrophobic interactions. Surfactant-induced healing produces high toughness (~1 MPa) gels withstanding 150 kPa of stress at a deformation ratio of 1,100 %. The healing technique developed here is generally applicable to the physical gels formed by hydrophobic associations.

**Keywords** Hydrogels · Self-healing · Hydrophobic associations · Toughness · Surfactant-induced healing

## Introduction

Self-healing is a common phenomenon observed in most biological materials such as skin, bones, and wood [1, 2]. The special ability of natural materials to heal cracks often

involves an energy dissipation mechanism due to the so-called sacrificial bonds that break and reform dynamically before the fracture of the molecular backbone [3]. Although synthetic hydrogels are very similar to biological tissues, they are normally very brittle and lack the ability to self-heal upon damage. To obtain a hydrogel with a high degree of toughness, one has to increase the overall viscoelastic dissipation along the gel sample by introducing dissipative mechanisms at the molecular level. A number of techniques for toughening of gels have recently been proposed including the double network gels [4], topological gels [5], nanocomposite hydrogels [6], and cryogels [7]. Moreover, to generate self-healing in synthetic hydrogels, different reversible molecular interactions have been used in the past few years, including hydrogen bonding [8–12], electrostatic interactions [13–15], molecular recognition [16–18], metal coordination [19, 20],  $\pi$ – $\pi$  stacking [21], dynamic chemical bonds [22–25], molecular diffusion [26, 27], and hydrophobic associations [28–32]. However, self-healing hydrogels synthesized so far suffer from low mechanical strength which may limit their use in any stress-bearing applications such as artificial cartilages.

Recently, we presented a simple strategy for the production of self-healing hydrogels via hydrophobic interactions [31, 32]. Large hydrophobes such as stearyl methacrylate (C18) could be copolymerized with the hydrophilic monomer acrylamide (AAm) in aqueous sodium dodecyl sulfate (SDS) solutions. This was achieved by the addition of salt (NaCl) into the reaction solution [31]. Salt leads to micellar growth and, hence, solubilization of large hydrophobes within the grown wormlike SDS micelles. Incorporation of hydrophobic sequences within the hydrophilic polyacrylamide (PAAm) chains via micellar polymerization technique generates strong hydrophobic interactions, which prevent dissolution of the physical gels in water, while the dynamic nature of the junction zones provides homogeneity and self-healing properties. It was shown that the hydrophobic associations surrounded by

A. Argun · M. P. Algi · O. Okay (✉)  
Department of Chemistry, Istanbul Technical University,  
34469 Istanbul, Turkey  
e-mail: okayo@itu.edu.tr

D. C. Tuncaboğlu  
Faculty of Pharmacy, Bezmialem Vakıf University,  
34093 Istanbul, Turkey

surfactant micelles act as reversible breakable cross-links, which are responsible for rapid self-healing of the hydrogels at room temperature without the need for any stimulus or healing agent [32].

However, when swollen in water, such hydrogels formed by hydrophobic associations behave similarly to chemically cross-linked ones with time-independent elastic moduli, a high degree of spatial inhomogeneity, and no self-healing ability upon damage. It was shown that the drastic structural change in the physical gels upon swelling in water is due to the extraction of SDS micelles from the gel network, leading to the loss of the reversible nature of the cross-linkages [32]. Thus, although mechanically strong and tough gels could be obtained after removal of surfactant, the resulting gels lose their ability to self-heal. This also prevents the application of self-healing hydrogels formed via hydrophobic interactions in aqueous environment.

Here, we report on the discovery that complete healing in the physical gels free of SDS micelles can be achieved by the treatment of the damaged area with an aqueous solution of wormlike SDS micelles. Healed hydrogels exhibit fracture stress of 150 kPa and a toughness of  $\sim 1$  MPa. We also show that the healing technique developed here is generally applicable to the physical gels formed by hydrophobic associations.

## Experimental

### Materials

Acrylamide (AAm, Merck), sodium dodecylsulfate (SDS, Sigma), ammonium persulfate (APS, Merck),  $N,N,N',N'$ -tetramethylethylenediamine (TEMED, Merck), and NaCl (Merck) were used as received. Commercially available stearyl methacrylate (C18, Fluka) consists of 65 % *n*-octadecyl methacrylate and 35 % *n*-hexadecyl methacrylate. Hydrogels were prepared by the micellar copolymerization of AAm with C18 at 24 °C for 24 h in the presence of an APS (3.5 mM)–TEMED (0.25 v/v%) redox initiator system. SDS

and NaCl concentrations were set to 7 w/v% (0.24 M) and 0.5 M, respectively. The total monomer concentration and the hydrophobe content of the monomer mixture were also fixed at 10 w/v% and 2 mol %, respectively. The gel preparation procedure was the same as in our previous studies [31, 32]. Shortly, SDS (0.7 g) was dissolved in 9.9 mL of aqueous solution of NaCl (0.2925 g) at 35 °C to obtain a transparent solution. Then, hydrophobic monomer C18 (0.0862 g) was dissolved in this SDS–NaCl solution under stirring for 2 h at 35 °C. After adding and dissolving AAm (0.9137 g) for 30 min, TEMED (25  $\mu$ L) was added into the solution. Finally, 0.1 mL of APS stock solution (0.8 g APS/10 mL distilled water) was added to initiate the reaction. The copolymerization reactions were carried out in plastic syringes of 4.7-mm internal diameters.

To obtain hydrogels free of SDS micelles, the gel samples were immersed in a large excess of water at 24 °C for at least 15 days by replacing water every second or third day to extract any soluble species. SDS concentration in the external solutions was estimated using the methylene blue method [31, 33]. A swelling time of about 8 days was needed to extract all SDS from the gels. The masses  $m$  of the gel samples were monitored as a function of swelling time by weighing the samples. Relative weight swelling ratio  $m_{\text{rel}}$  of gels was calculated as  $m_{\text{rel}} = m/m_0$ , where  $m_0$  is the initial mass of the gel sample. Then, the equilibrium swollen gel samples were taken out of water and immersed in liquid nitrogen for 5 min before they were freeze-dried. The gel fraction  $W_g$ , that is, the conversion of monomers to the cross-linked polymer (mass of water-insoluble polymer/initial mass of the monomer) was calculated from the masses of dry, extracted polymer network and from the comonomer feed.

### Uniaxial compression measurements

The measurements were performed in a thermostated room at  $24 \pm 0.5$  °C on cylindrical hydrogel samples of 4.7 mm in diameter and  $5.3 \pm 0.3$  mm in length. The uniaxial compression measurements were performed on a Zwick Roell test machine using a 500-N load cell. The hydrogel sample was

**Fig. 1** Stress–strain curves of the hydrogels with **a** and without SDS **b** as the dependence of nominal  $\sigma_{\text{nom}}$  (open symbols) and true  $\sigma_{\text{true}}$  stresses (filled symbols) on the deformation ratio  $\lambda$

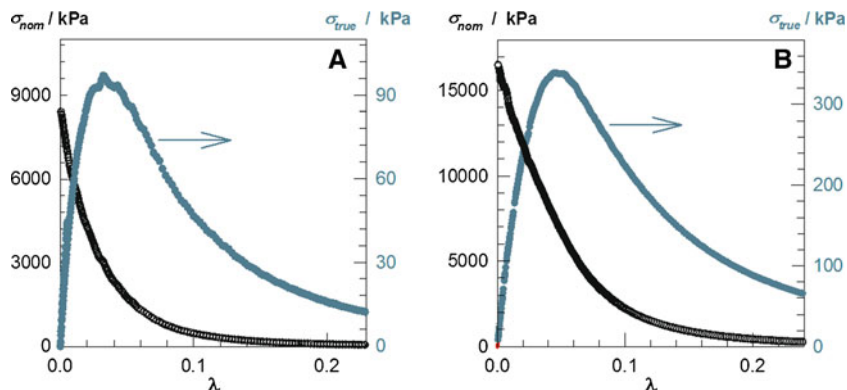


**Table 1** Properties of the physical gels with and without SDS

SDS (%)	Self-healing efficiency (%)	Elongation				Compression			
		$E/\text{kPa}$	$\sigma_f/\text{kPa}$	$\lambda_f$	$W/\text{kJ m}^{-3}$	$E/\text{kPa}$	$\sigma_f/\text{MPa}$	$\lambda_f$	$W/\text{kJ m}^{-3}$
7	100	8 (2)	16 (3)	18 (2)	136 (24)	5 (1)	2.7 (0.3)	0.037 (0.006)	70 (16)
0	0	32 (4)	138 (15)	8 (1)	580 (140)	30 (2)	8.6 (0.6)	0.044 (0.002)	450 (22)

Standard deviations are in parentheses

$E$  Young's modulus,  $\sigma_f$  fracture stress,  $\lambda_f$  deformation ratio to break,  $W$  toughness

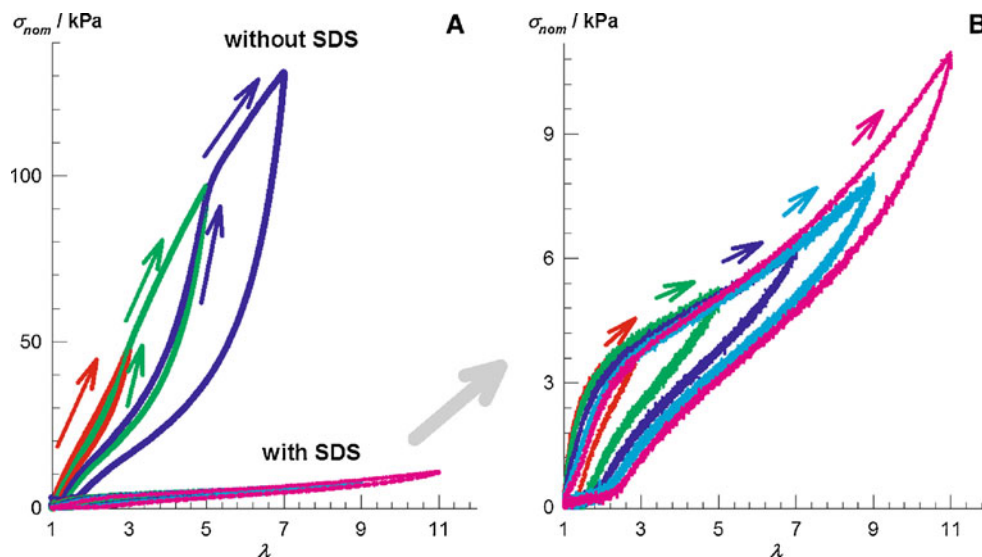
placed between the plates of the instrument. Before the test, an initial compressive contact to  $0.004 \pm 0.003$  N was applied to ensure a complete contact between the gel and the plates. The tests were conducted at a strain rate of  $1.6 \times 10^{-3} \text{ s}^{-1}$  (0.5 mm/min). Load and displacement data were collected during the experiment. Compressive stress is presented by its nominal  $\sigma_{\text{nom}}$  and true values  $\sigma_{\text{true}} (= \lambda \sigma_{\text{nom}})$ , which are the forces per cross-sectional area of the undeformed and deformed gel specimen, respectively, while the strain is given by  $\lambda$ , the deformation ratio (deformed length/initial length). Compressive modulus was calculated from the slope of stress–strain curves between 5 and 15 % compressions. At large compressions, failure was not easily observed in the hydrogels because the nominal stress  $\sigma_{\text{nom}}$  did not decrease after the samples broke. This is illustrated in Fig. 1 showing the stress–strain curves of the hydrogels with and without SDS under compression as the dependence of nominal  $\sigma_{\text{nom}}$  and true  $\sigma_{\text{true}}$  stresses on the deformation ratio  $\lambda$ . Although  $\sigma_{\text{nom}}$  increases continuously with increasing strain,  $\sigma_{\text{true}} - \lambda$  plots pass through maxima due to the onset of failure in the gel specimen. Note that the brittle gel samples prepared in the presence of a chemical cross-linker suddenly fractured during the compression tests so that the failure occurred at the maxima of

$\sigma_{\text{true}} - \lambda$  plots. The behavior of the present gels was a consequence of the sample breaking into several pieces that still supported the stress. The fracture stress  $\sigma_f$  and the compression ratio at break  $\lambda_f$  were calculated from the maxima in  $\sigma_{\text{true}} - \lambda$  plots taken as the fracture point of the gel samples.

### Uniaxial elongation measurements

The measurements were performed on cylindrical hydrogel samples of 4.7 mm in diameter on a Zwick Roell test machine using a 10-N load cell under the following conditions: strain rate =  $0.075 \text{ s}^{-1}$  (50 mm/min), sample length between jaws =  $11 \pm 1$  mm. Samples were held on the test machine between clamps altered with antislip tape (Tesa,  $25 \times 15$  mm) together with cyanoacrylate adhesive (Evobond), or with wood strips to better grip the slippery gel samples. The fracture stress, elongation ratio at break, and toughness were recorded. Tensile modulus was calculated from the slope of stress–strain curves between elongations of 5 and 15 %. Cyclic elongation tests were conducted at a constant crosshead speed of 50 mm/min to a maximum elongation ratio, followed by retraction to zero force and a waiting time of 7 min, until the next cycle of elongation. All the gel samples recovered their original

**Fig. 2** Successive loading/unloading cycles for the physical gels with and without SDS. Panel **b** is a zoom-in view of the data of gels containing SDS



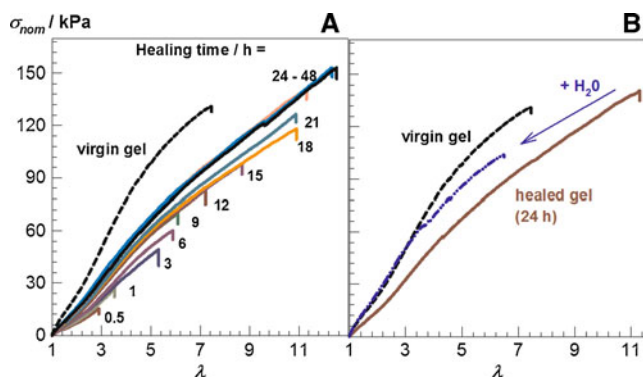


**Fig. 3** Stress–strain curves of the virgin gel sample without SDS (*dashed curve*) and the healed gel samples (*solid curves*). Healing times are indicated. The *blue (dash-dot)* curve in panel **b** represents the stress–strain data of a gel sample healed for 24 h, which was then immersed into an excess of water for 2 weeks to extract SDS prior to the mechanical tests

lengths after 7 min of relaxation time. For reproducibility, at least six samples were measured for each gel, and the results were averaged.

## Results and discussion

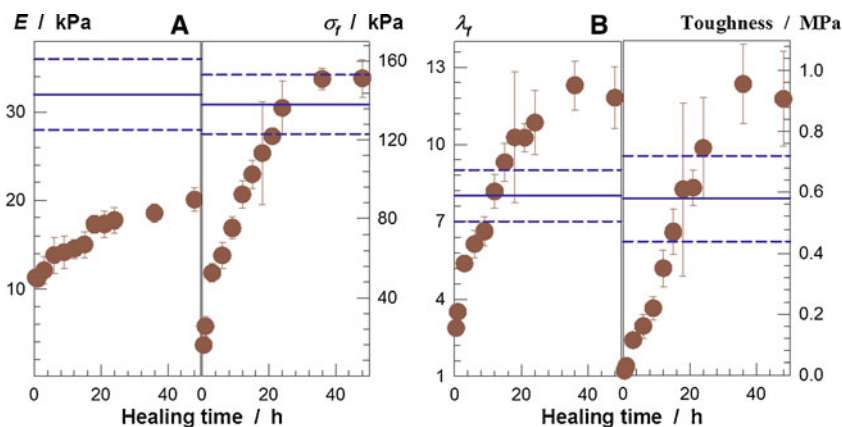
Physical gels were prepared by the micellar copolymerization of AAm with 2 mol % C18 at 24 °C in aqueous SDS–NaCl solutions. To obtain physical gels free of SDS micelles, the gel samples were extracted in water at 24 °C. The gel fraction (mass of water-insoluble polymer/initial mass of the monomer) was above 0.90, while the weight swelling ratio of the gels with respect to the state of preparation was close to unity. In this way, two types of physical gels of the same polymer concentration (10 w/v %) and composition (2 mol % C18 and the rest being AAm units) were obtained, one containing 7 w/v % SDS and the other free of SDS, which will be called hereafter gels with and without SDS, respectively.

The mechanical characteristics of the physical gels with and without SDS are collected in Table 1. The tensile and

compressive moduli  $E$  of the physical gel increase 4- and 6-fold, respectively, upon removal of the surfactant from the gel network. The gel containing SDS ruptures when stretched to about 18 times its original length, while the same gel without SDS ruptures at  $\lambda_f = 8 \pm 1$ . Moreover, the gel with SDS fails upon application of  $16 \pm 3$  kPa compressive stress whereas that without SDS withstands about 9-fold larger fracture stress and exhibits about 5-fold larger toughness. Thus, the mechanical strength of the physical gel is significantly improved after its swelling in water, i.e., after extraction of SDS micelles from the physical network. This is, as detailed before, due to the weakening of hydrophobic interactions in the presence of surfactants [32].

The large strain properties of the gels were compared by cyclic elongation tests conducted up to a strain below the failure. In Fig. 2a, successive loading–unloading cycles of the gel samples with and without SDS are shown as the dependence of the nominal stress  $\sigma_{nom}$  on the deformation ratio  $\lambda$ . Figure 2b is a zoom-in view of the data of gels containing SDS. For clarity, successive cycles are presented by curves with different colors, and the loading curves are indicated by up-pointing arrows. The tests were carried out by first elongating the gel samples to a maximum strain  $\lambda_{max,1}$  and then unloading. After a wait time of 7 min, the samples were again loaded and elongated to an increasing maximum strain  $\lambda_{max,2}$  and unloaded. These successive tensile cycles were carried out several times with increasing maximum strain up to  $\lambda_{max,n} = 11$  and 7 for gels with and without SDS, respectively. For the gel with SDS (Fig. 2b), the  $n$ th loading curve is always overlapped by the  $(n-1)$ th loading curve over the whole range of  $\lambda_{max,n}$ . The perfect superposition of the successive loading curves up to 1,000 % of elongation ratio reveals that the damage done to the gel sample during the loading cycle is recoverable in nature, and the bonds broken during elongation are reformed after a wait time of 7 min. In contrast, the gel without SDS exhibits irreversibility (Fig. 2a), i.e.,  $n$ th loading curve follows the path of the unloading curve of the previous cycle up to its maximum strain  $\lambda_{max,n-1}$ . This

**Fig. 4** Young's modulus  $E$ , fracture stress  $\sigma_f$ , elongation ratio  $\lambda_f$  at break, and toughness of healed gels shown as a function of the healing time. The *solid lines* represent the behavior of virgin gel sample without SDS, and the *dashed lines* are the standard deviations



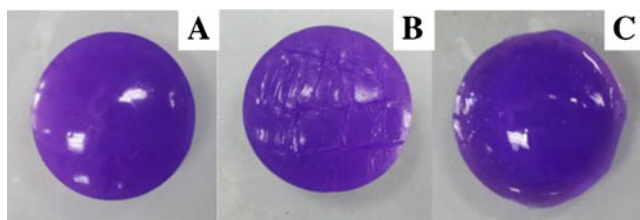


**Fig. 5** Healing of a surface scratch in the gel containing no SDS. The gel was colored using a dye for easy visualization. **a** Virgin surface of the gel. **b** After making scratches (about 2 mm deep) on the surface of the gel. **c** The surface of the gel after spraying the healing agent and after a healing time of 24 h

indicates the occurrence of an irreversible damage during the previous cycle, while additional damage only occurs at a higher maximum strain.

In accord with the cyclic test results, the weak gels with SDS exhibited a self-healing efficiency of nearly 100 % after a healing time of 60 min [32]. However, no such self-healing behavior was observed in mechanically strong gels without SDS. This suggests that the key factor leading to the self-healing is the weakening of strong hydrophobic interactions due to the presence of surfactant molecules. We tried to induce healing in the physical gels free of SDS micelles by the treatment of the cut surfaces with surfactant solutions. For this purpose, cylindrical gel samples of about 5 mm in diameter and 6 cm in length were cut in the middle, and the cut regions were immersed (5 mm deep) into an aqueous 7 w/v % SDS solution for 10 min. Then, the two halves were merged together within a plastic syringe (of the same diameter as the gel sample) at 24 °C by slightly pressing the piston plunger. The healing time was varied from 10 min to 12 days, and each experiment was carried out starting from a virgin sample. No healing could be achieved in the hydrogels even at elevated temperatures (up to 60 °C). This is attributed to the presence of small SDS micelles in the surfactant solution that cannot solubilize large hydrophobic sequences locating in the cut surfaces. However, 7 w/v % SDS solution prepared in 0.5 M NaCl induced a significant healing in a short period of time.

Since the aggregation number of SDS micelles in 0.5 M NaCl is about 200, as compared to 60 for the minimum spherical SDS micelle [32], this suggests that the grown micelles in the healing agent are able to solubilize the hydrophobes in the cut surfaces. Indeed, it was observed that the cut surfaces immersed in SDS–NaCl solutions start to liquefy after a few minutes, so that the hydrophobes can easily find their partners in the other cut surface due to the hydrophobic interactions.

In Fig. 3a, stress–strain curves of the virgin gel sample without SDS (dashed curve) and the healed gel samples (solid curves) are shown. The fracture stress after 1 h of healing is  $25 \pm 5$  kPa which is close twice the fracture stress of the virgin gel sample containing SDS (Table 1). For healing times ranging from 30 min to 9 h, we observed that the healed region of gels is more swollen as compared to the bulk region. This is expected, given that the absorption of SDS by the polymer at the welded interface produces an excess of counterion concentration inside the gel and leads to increased gel swelling [31]. This interface also acts as a weak point in the healed gels so that they always rupture at this region. However, for longer healing times (>9 h), the welded interface deswells again and becomes identical to the bulk region; simultaneously, the healed gel samples rupture in the bulk region, while the welded interface remains unbroken. For all healing times indicated in Fig. 3a, the surfactant-mediated healing is irreversible: When immersed in water to extract the healing agent (SDS + NaCl), the healed gel samples remain stable as the virgin ones.

The mechanical characteristics of the healed gel samples are plotted in Fig. 4 against the healing time. The horizontal solid lines represent the characteristics of the virgin sample listed in the second row of Table 1 with standard deviations indicated by the dashed lines. Both the fracture stress  $\sigma_f$  and the elongation at break  $\lambda_f$  of the gel samples rapidly increase with increasing healing time, and after 20 h, they reach to the values of the virgin gel sample. For longer healing times, the healed gel samples become stronger and tougher than the original gel. However, the modulus  $E$  of healed gels partially

**Table 2** Tensile strength and elongations to break of healed hydrogels formed via different reversible molecular interactions

Healing process	Healing type	Tensile strength (healing time)	Elongation to break	Reference
Hydrophobic interactions	Self	0.1 kPa (10 s)	–	[29]
	Self	30 kPa (3 days)	11	[28]
	Self	20–40 kPa (30 min)	13–17	[32, 35]
	Surfactant-induced	150 kPa (24 h)	12	Present work
H-bonding	pH-induced	35 kPa (24 h)	–	[8]
	Self	~100 kPa (24 h)	4	[9]
	Self (graphene oxide composite hydrogel)	200–350 kPa (24 h)	25–48	[11]
	Self (nanocomposite hydrogel)	130 kPa (30 min)	12	[12]
Dynamic chemical bonds	Self	300 kPa (24 h)	5	[22]

recovers its original value, and about 63 % of healing efficiency in terms of the recovered modulus was obtained after 50 h. We attribute this behavior to the presence of SDS in the healed gel samples weakening hydrophobic interactions. Indeed, when the healed samples are immersed into an excess of water to extract SDS micelles, their stress–strain curves approach to the curve of the virgin sample. This behavior is illustrated by the blue (dash-dot) curve in Fig. 3b representing the stress–strain data of a gel sample healed for 24 h, which was then immersed into an excess of water for 2 weeks to extract SDS prior to the mechanical tests. Both the fracture stress and the elongation at break are 80 % of the original values. Experiments also showed that increasing temperature during healing further increases the efficiency of healing. For instance, fixing the healing time at 6 h while increasing the healing temperature from 25 to 60 °C leads to an increase in the fracture stress of healed hydrogels from 60 to 90 kPa. The increasing ability of the hydrogels to self-heal at a high temperature is ascribed to a decrease of the lifetime of hydrophobic associations, as already observed in semi-dilute solutions of hydrophobically modified PAAms [34].

The healing technique developed here is applicable to the physical gels formed by hydrophobic associations. PAAm hydrogels formed using 2 mol % *n*-alkyl (meth)acrylates of various alkyl chain lengths between 12 and 22 carbon atoms as the physical cross-linker, as we reported before [35], could be healed using the SDS–NaCl solution. This technique thus overcomes the necessity of the presence of surfactant micelles in the gels for their healing and, therefore, opens their applications in the aqueous environment. To demonstrate the application of the hydrogels as healing coatings, artificial scratches about 2 mm deep were created on the gel surfaces (Fig. 5). A complete healing was achieved by spraying the cracks with the SDS–NaCl solution after a healing time of 24 h.

## Conclusions

We have demonstrated that the physical gels formed via hydrophobic interactions can be healed using aqueous solutions of wormlike surfactants. Since the hydrogels formed by large hydrophobes as a physical cross-linker have long-lived associations [32, 35], the polymer chains cannot diffuse to the damaged area to heal the broken gel sample. As a consequence, healing needs an external stimulus to facilitate the diffusion of polymer chains, so that the broken associations are able to reform their original structure. The results show that healing induced by wormlike SDS micelles produces gels of high toughness (~1 MPa) withstanding 150 kPa of stress at a deformation ratio of 1,100 %. Table 2 summarizes the tensile strength and elongation to break of healed hydrogels formed via different reversible molecular interactions. Present

hydrogels exhibit the highest mechanical strength ever reported for gels formed by hydrophobic associations. We propose that the nanoparticles included into the physical network of the present hydrogels would further increase the mechanical performance of healed hydrogels.

**Acknowledgments** MPA acknowledges the financial support from the Scientific and Technical Research Council of Turkey (TUBITAK) for a postdoctoral scholarship. This work was supported by TUBITAK, TBAG–109T646. OO thanks the Turkish Academy of Sciences (TUBA) for the partial support.

## References

- Fratzl P (2007) *J R Soc Interface* 4:637–642
- Hamilton AR, Sottos NR, White SR (2010) *Adv Mater* 22:5159–5163
- Fantner GE, Oroudjev E, Schitter G, Golde LS, Thurner P, Finch MM, Turner P, Gutschmann T, Morse DE, Hansma H, Hansma PK (2006) *Biophys J* 90:1411–1418
- Gong JP, Katsuyama Y, Kurokawa T, Osada Y (2003) *Adv Mater* 15: 1155–1158
- Okumura Y, Ito K (2001) *Adv Mater* 13:485–487
- Haraguchi K, Takehisa T (2002) *Adv Mater* 14:1120–1124
- Ceylan D, Okay O (2007) *Macromolecules* 40:8742–8749
- Phadke A, Zhang C, Arman B, Hsu C-C, Mashelkar RA, Lele AK, Tauber MJ, Arya G, Varghese S (2012) *PNAS* 109:4383–4388
- Zhang H, Xia H, Zhao Y (2012) *ACS Macro Lett* 1:1233–1236
- Cui J, del Campo A (2012) *Chem Commun* 48:9302–9304
- Liu J, Song G, He C, Wang H (2013) *Macromol Rapid Commun* 34: 1002–1007
- Haraguchi K, Uyama K, Tanimoto H (2011) *Macromol Rapid Commun* 32:1253–1258
- Sun J-Y, Zhao X, Illeperuma WRK, Chaudhuri O, Oh KH, Money DJ, Vlassak JJ, Suo Z (2012) *Nature* 489:133–136
- South AB, Lyon LA (2010) *Angew Chem Int Ed* 49:767–771
- Wang Q, Mynar JL, Yoshida M, Lee E, Lee M, Okura K, Kinbara K, Aida T (2010) *Nature* 463:339–343
- Appel EA, Biedermann F, Rauwald U, Jones ST, Zayed JM, Scherman OA (2010) *J Am Chem Soc* 132:14251–14260
- Foo CTSWP, Lee JS, Mulyasmita W, Parisi-Amon A, Heilshorn SC (2009) *PNAS* 106:22067–22072
- Skrzeszewska PJ, Sprakel J, Wolf FA, Fokkink R, Stuart MAC, van de Gucht J (2010) *Macromolecules* 43:3542–3548
- Holtén-Andersen N, Harrington MJ, Birkedal H, Lee BP, Messersmith PB, Lee KYC, Waite JH (2011) *PNAS* 108:2651–2655
- Shafiq Z, Cui J, Pastor-Perez L, San Miguel V, Gropeanu RA, Serrano C, del Campo A (2012) *Angew Chem Int Ed* 124:4408–4411
- Xu Y, Wu Q, Sun Y, Bai H, Shi G (2010) *ACS Nano* 4:7358–7362
- Liu F, Li F, Deng G, Chen Y, Zhang B, Zhang J, Liu C-Y (2012) *Macromolecules* 45:1636–1645
- Deng G, Tang C, Li F, Jiang H, Chen Y (2010) *Macromolecules* 43: 1191–1194
- Zhang Y, Tao L, Li S, Wei Y (2011) *Biomacromolecules* 12:2894–2901
- He L, Fullenkamp DE, Rivera JG, Messersmith PB (2011) *Chem Commun* 47:7497–7499
- Fromowicz P, Klinger D, Landfester K (2011) *Chem Eur J* 17: 12465–12475
- Quint SB, Pacholski C (2011) *Soft Matter* 7:3735–3738
- Jiang G, Liu C, Liu X, Zhang G, Yang M, Chen Q, Liu F (2010) *J Macromol Sci A* 47:335–342

29. Hao X, Liu H, Xie Y, Fang C, Yang H (2013) *Colloid Polym Sci* 291: 1749–1758
30. Hao J, Weiss RA (2011) *Macromolecules* 44:9390–9398
31. Tuncaboylu DC, Sari M, Oppermann W, Okay O (2011) *Macromolecules* 44:4997–5005
32. Tuncaboylu DC, Sahin M, Argun A, Oppermann W, Okay O (2012) *Macromolecules* 45:1991–2000
33. ISO (1996) Water quality. Determination of surfactants. Part 1: determination of anionic surfactants by measurement of the methylene blue index (MBAS). ISO 7875-1, ISO/TC 147. ISO, Geneva
34. Volpert E, Selb J, Candau F (1998) *Polymer* 39:1025–1033
35. Tuncaboylu DC, Argun A, Sahin M, Sari M, Okay O (2012) *Polymer* 53:5513–5522